# Supplementary Materials: Rethinking IoU-based Optimization for Single-stage 3D Object Detection

Hualian Sheng[1,2,3], Sijia Cai[2], Na Zhao[3⋆], Bing Deng[2], Jianqiang Huang[2], Xian-Sheng Hua[2], Min-Jian Zhao[1], and Gim Hee Lee[3]

[1] College of Information Science and Electronic Engineering, Zhejiang University
[2] Alibaba Cloud Computing Ltd.
[3] Department of Computer Science, National University of Singapore
{hlsheng,mjzhao}@zju.edu.cn, {nazhao, gimhee.lee}@comp.nus.edu.sg,
{stephen.csj, dengbing.db, jianqiang.hjq, xiansheng.hxs}@alibaba-inc.com

Some supplementary materials are provided to further validate the proposed approach. The supplementary materials include ablation studies on parameter $k$, more comparisons to existing ODIoU loss [9] and 3D IoU loss [10], inserting RDIoU into state-of-the-art 3D detectors, and visualization results, respectively.

**Effect of parameter $k$.** As shown in Table 1, we try different settings of the edge $k$ to control the weight of rotation change. Here, we can see that $k$ is an important factor to boost the final performance, and $k = 1.0$ is the best.

| $k$ | 0.6 | 0.8 | **1.0** | 1.2 | 1.4 | 1.6 | 1.8 |
|---|---|---|---|---|---|---|---|
| $3\text{D}_{R40}$ | 85.89 | 85.96 | **86.20** | 85.92 | 85.85 | 85.70 | 85.59 |

**Table 1.** Ablation study on parameter $k$, which reflects the sensitivity of RDIoU value to the rotation difference.

**More comparison with 3D IoU [10] and ODIoU [9].** In Table 2, we provide more comparison results for 3D IoU and ODIoU with our proposed RDIoU. It can be seen that RDIoU outperforms both 3D IoU and ODIoU by large margins.

**Inserting RDIoU into state-of-the-art methods.** We reproduce SOTA single-stage methods: CIA-SSD[8], SA-SSD[2], SE-SSD[9], and two-stage methods: PV-RCNN[5], Voxel-RCNN[1], CT3D[4] in Table 3. Our RDIoU can significantly improve their performance, especially for the single-stage detectors.

**Visualization.** We provide some qualitative detection results on KITTI *test* set in Figure 1, it shows that RDIoU can produce high-quality 3D bounding boxes in diversified scenarios.

⋆ Corresponding author

| Method | Easy ($3D_{R11}$) | Mod. ($3D_{R11}$) | Hard ($3D_{R11}$) | Mod. ($3D_{R40}$) |
|---|---|---|---|---|
| PointPillar[3] | 87.08 | 77.74 | 76.24 | 79.88 |
| PointPillar (+3D IoU) | 86.91 | 77.93 | 76.83 | 80.12 |
| PointPillar (+ODIoU) | 87.15 | 78.29 | 77.08 | 80.58 |
| PointPillar (+RDIoU) | **88.89** | **78.89** | **78.02** | **82.42** |
| SECOND[7] | 88.78 | 78.74 | 77.51 | 82.85 |
| SECOND (+3D IoU) | 88.04 | 80.97 | 77.06 | 83.02 |
| SECOND (+ODIoU) | 88.69 | 82.82 | 77.41 | 83.88 |
| SECOND (+RDIoU) | **89.24** | **86.10** | **78.60** | **85.80** |
| CT-stacked | 88.93 | 78.91 | 77.63 | 83.01 |
| CT-stacked (+3D IoU) | 88.23 | 81.09 | 77.16 | 83.29 |
| CT-stacked (+ODIoU) | 88.70 | 82.89 | 77.53 | 84.01 |
| CT-stacked (+RDIoU) | **89.76** | **86.62** | **79.04** | **86.20** |

**Table 2.** Comparisons to 3D IoU and ODIoU.

| Type | Method | Easy ($3D_{R11}$) | Mod. ($3D_{R11}$) | Hard ($3D_{R11}$) | Mod. ($3D_{R40}$) |
|---|---|---|---|---|---|
| Single-stage | CIA-SSD[8] | **89.48** | 78.54 | 77.35 | 81.93 |
| | CIA-SSD (+RDIoU) | 89.07 | **85.44** | **78.55** | **85.23** |
| | SA-SSD[2] | 89.26 | 79.28 | 78.35 | 82.65 |
| | SA-SSD (+RDIoU) | **89.56** | **86.04** | **78.76** | **85.87** |
| | SE-SSD[9] | 89.07 | 79.22 | 78.37 | 82.48 |
| | SE-SSD (+RDIoU) | **89.24** | **85.98** | **78.60** | **85.24** |
| Two-stage | PV-RCNN[5] | 89.31 | 84.49 | 78.78 | 84.93 |
| | PV-RCNN (+RDIoU) | **89.47** | **86.21** | **79.01** | **85.96** |
| | Voxel-RCNN[1] | 89.44 | 84.45 | 78.90 | 85.24 |
| | Voxel-RCNN (+RDIoU) | **89.67** | **86.12** | **78.91** | **85.92** |
| | CT3D[4] | **89.54** | 86.06 | **78.99** | 85.82 |
| | CT3D (+RDIoU) | 89.31 | **86.27** | 78.90 | **85.94** |

**Table 3.** Inserting our RDIoU into SOTA methods based on OpenPCDet[6].

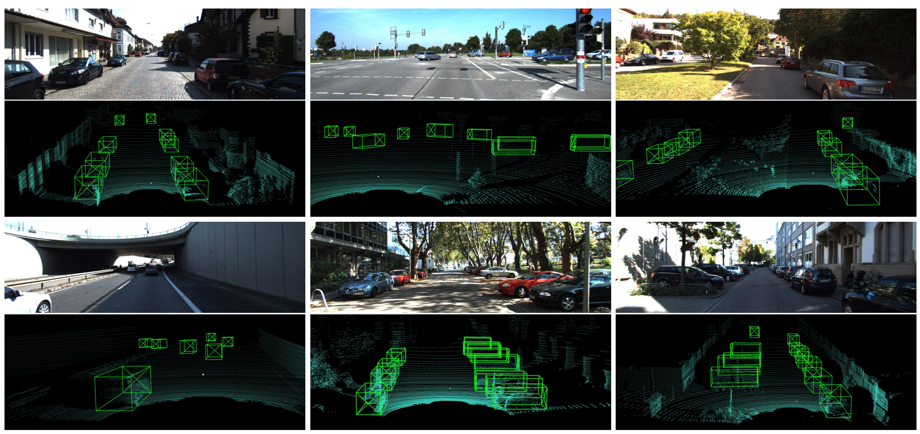

**Fig. 1.** Snapshots of qualitative results on KITTI test set. The output 3D bounding boxes are shown in green.

## References

1. Deng, J., Shi, S., Li, P., Zhou, W., Zhang, Y., Li, H.: Voxel r-cnn: Towards high performance voxel-based 3d object detection. arXiv preprint arXiv:2012.15712 (2020) 1
2. He, C., Zeng, H., Huang, J., Hua, X.S., Zhang, L.: Structure aware single-stage 3d object detection from point cloud. In: Proceedings of the IEEE/CVF Conference on Computer Vision and Pattern Recognition (CVPR). pp. 11873–11882 (2020) 1
3. Lang, A.H., Vora, S., Caesar, H., Zhou, L., Yang, J., Beijbom, O.: Pointpillars: Fast encoders for object detection from point clouds. In: Proceedings of the IEEE/CVF Conference on Computer Vision and Pattern Recognition (CVPR). pp. 12697–12705 (2019) 1
4. Sheng, H., Cai, S., Liu, Y., Deng, B., Huang, J., Hua, X.S., Zhao, M.J.: Improving 3d object detection with channel-wise transformer. In: Proceedings of the IEEE/CVF International Conference on Computer Vision (ICCV). pp. 2743–2752 (2021) 1
5. Shi, S., Guo, C., Jiang, L., Wang, Z., Shi, J., Wang, X., Li, H.: Pv-rcnn: Point-voxel feature set abstraction for 3d object detection. In: Proceedings of the IEEE/CVF Conference on Computer Vision and Pattern Recognition (CVPR). pp. 10529–10538 (2020) 1
6. Team, O.D.: Openpcdet: An open-source toolbox for 3d object detection from point clouds. `https://github.com/open-mmlab/OpenPCDet` (2020) 3
7. Yan, Y., Mao, Y., Li, B.: Second: Sparsely embedded convolutional detection. Sensors **18**(10), 3337 (2018) 1
8. Zheng, W., Tang, W., Chen, S., Jiang, L., Fu, C.W.: Cia-ssd: Confident iou-aware single-stage object detector from point cloud. arXiv preprint arXiv:2012.03015 (2020) 1
9. Zheng, W., Tang, W., Jiang, L., Fu, C.W.: Se-ssd: Self-ensembling single-stage object detector from point cloud. In: Proceedings of the IEEE/CVF Conference on Computer Vision and Pattern Recognition (CVPR). pp. 14494–14503 (2021) 1, 1, 1
10. Zhou, D., Fang, J., Song, X., Guan, C., Yin, J., Dai, Y., Yang, R.: Iou loss for 2d/3d object detection. In: International Conference on 3D Vision (3DV). pp. 85–94. IEEE (2019) 1, 1